energies

MDPI

Article

Production of Fuel Range Hydrocarbons from Pyrolysis of Lignin over Zeolite Y, Hydrogen

Ghulam Ali [1], Marrij Afraz [1], Faisal Muhammad [1], Jan Nisar [1,*], Afzal Shah [2,*], Shamsa Munir [3] and Syed Tasleem Hussain [4]

[1] National Centre of Excellence in Physical Chemistry, University of Peshawar, Peshawar 25120, Pakistan
[2] Department of Chemistry, Quaid-i-Azam University, Islamabad 45320, Pakistan
[3] School of Applied Sciences and Humanities, National University of Technology (NUTECH), Islamabad 44000, Pakistan
[4] Department of Chemistry, Kohat University of Science and Technology (KUST), Kohat 26000, Pakistan
* Correspondence: pashkalawati@gmail.com or jan_nisar@uop.edu.pk (J.N.); afzalshah@qau.edu.pk or afzals_qau@yahoo.com (A.S.)

Abstract: In the current study, plain and lignin loaded with Zeolite Y, hydrogen was decomposed in a pyrolysis chamber. The reaction parameters were optimized and 390 °C, 3% catalyst with a reaction time of 40 min were observed as the most suitable conditions for better oil yield. The bio-oil collected from the catalyzed and non-catalyzed pyrolytic reactions was analyzed by gas chromatography mass spectrometry (GCMS). Catalytic pyrolysis resulted in the production of bio-oil consisting of 15 components ranging from C_3 to C_{18} with a high percentage of fuel range benzene derivatives. Non-catalytic pyrolysis produced bio-oil that consists of 58 components ranging from C_3 to C_{24}; however, the number and quantity of fuel range hydrocarbons were lower than in the catalyzed products. The pyrolysis reaction was studied kinetically for both samples using thermogravimetry at heating rates of 5, 10, 15 and 20 °C/min in the temperature range 20–600 °C. The activation energies and pre-exponential factors were calculated using the Kissinger equation for both non-catalytic and catalytic decomposition and found to be 157.96 kJ/mol, 141.33 kJ/mol, 2.66×10^{13} min^{-1} and 2.17×10^{10} min^{-1}, respectively. It was concluded that Zeolite Y, hydrogen worked well as a catalyst to decrease activation energy and enhance the quality of the bio-oil generated.

Keywords: lignin; zeolite Y; hydrogen; pyrolysis; GC/MS; kinetics; activation energy

Citation: Ali, G.; Afraz, M.; Muhammad, F.; Nisar, J.; Shah, A.; Munir, S.; Tasleem Hussain, S. Production of Fuel Range Hydrocarbons from Pyrolysis of Lignin over Zeolite Y, Hydrogen. *Energies* **2023**, *16*, 215. https://doi.org/10.3390/en16010215

Academic Editors: Shie Jelueng and Min-Hao Yuan

Received: 13 November 2022
Revised: 13 December 2022
Accepted: 19 December 2022
Published: 25 December 2022

1. Introduction

Non-renewable fossil resources are facing a serious challenge and their excessive use and over consumption due to the increasing population growth is leading to their depletion. Moreover, the global energy demand based on fossil fuels has a negative impact on the environment; therefore, there is an intense need for more efficient and environmentally friendly alternative energy resources on large scale [1]. Climate change and other environmental issues are produced as a result of excessive use of fossil fuels as their combustion causes emissions of unburnt particles, carbon dioxide and other compounds resulting in the greenhouse effect and global warming [2,3]. Moreover, fossil fuel such as coal have some sulphur content and its burning causes emission of sulphur dioxide that contributes to acid rain, which causes water pollution [4]. Therefore, we must use renewable energy sources to address all these issues, which is the preferable alternative for meeting growing energy demand. The use of renewable energy has greatly influenced human activities and has a vast application in the energy sector. It is becoming the most valued alternative for fossil-based energy [5]. Biomass, sunlight, wind, hydro and geothermal are some important sources of renewable energy [6], and the focus of researchers on using renewable energy is increasing with increase in energy demand as it is a cheap and pollution free source [7].

Zeolite is a solid material, and its use as catalyst is often preferred as the separation of solid catalyst is comparatively easy after the reaction [8]. Due to its high activity and durability, zeolite has been found to be a specialized catalyst for enhancing bio aromatic production. Moreover, it is preferred over oxides, heteropoly acids, and various transition metals due to its resistance to various catalytic poisons created during reactions. Zeolites have unique structural and acidic qualities that lengthen their lifespan and improve their selectivity for various gasoline hydrocarbons [9]. Zeolites have been extensively used for the conversion of waste biomass to bio-oil; however, a few studies have reported on the utilization of zeolite for decomposition of lignin. Decomposition kinetics of lignin has been studied by a few research workers. Jiang et al. [10] studied the kinetic of decomposition of four different types of lignin obtained from various sources using the Kissinger method and observed that the activation energy is dependent on the plant from which the lignin was obtained and the separation method used.

Sharma et al. [11] performed pyrolysis of lignin and char and characterized the pyrolysates obtained under different conditions. The high yield of char was assigned to the existence of inorganic components, and the removal of these components led to a decrease in char yield. It was revealed from the experiment that lignin char has low reactivity in comparison with the char obtained from other biomass components.

Kawamoto [12] presented a detailed review on lignin conversion into different components via pyrolysis. However, there are still discrepancies in understanding the mechanism of lignin pyrolysis and more experimental and theoretical work needs to be done to explain the reaction mechanism.

Mu et al. [13] reviewed the pyrolysis of lignin and observed that the mechanism of lignin pyrolysis is completely different to that of other biomass components, i.e., cellulose and hemicellulose. The authors focused on recent advancements on the pyrolysis of lignin, degradation mechanisms, catalytic and non-catalytic reactions, and upgradation of bio-oil. Though the products obtained from lignin pyrolysis have been proved to be of commercial importance, there are still many problems to be solved.

Liu et al. [14] used Van Soest's method for extracting lignin from two different biomass samples and studied the mechanism of pyrolysis. FTIR was used for characterization of the products formed. The major volatile products were phenols along with alcohols, aldehydes and some forms of acids. The gaseous fraction was found to compose of CO, CO_2 and methane. However, further research using advanced analytical techniques is necessary to ascertain the exact mechanism of the pyrolysis reaction.

Lignin, with chemical formula $C_{81}H_{92}O_{28}$, is a stiff, aromatic, amorphous and hydrophobic biopolymer. One portion of lignin is found inside the cell wall, while the other portion is found between the cells in the intermediate lamella [15]. Lignin is bonded with the hemicellulose through covalent linkages and provide stiffness and strength to the plant cell wall [16]. Wood contains 25–40% lignin [17]. Lignin sources are widely available all around the world that include cotton, wood pulp, paper industries and different other plant materials [18].

The large-scale production of lignin in pulp and paper industries has a great potential to be converted into useful products such as bio-oils. This unnecessary waste lignin can be utilized for conversions to biofuel which will encourage the proper use of waste lignin [19]. Moreover, it is cost effective, non-polluting and efficient energy source [20]. Therefore, the major focus of present research is to analyze the kinetics of thermal and thermo-catalytic decomposition of lignin. The pyrolysis process was performed in an in-house designed furnace at a wide temperature range, and the liquid fuel collected with/without Zeolite Y, hydrogen was analyzed by GC/MS. For kinetic study, lignin was subjected to thermal and thermo-catalytic degradation using thermogravimetry. Kissinger equation was applied to examine the kinetic parameters of the decomposition reaction. The data obtained from these experiments will help in the utilization of lignin for production of useful products.

2. Material and Methods

2.1. Materials

In the recent study, lignin used was an alkali lignin (CAS: 8068-05-1) with low sulphonates content that was purchased from Aldrich Chemistry, USA. The Aldrich alkali lignin was chosen for this investigation because it is commercially accessible and comes in a highly purified form with a low moisture content (5%). It was in the form of brown powder with a pH of 10.5 (3 wt.%) and is water soluble. The Zeolite Y, hydrogen (CAS: 1318-02-1) used in this study as a catalyst was purchased from Alfa Aesar GmbH & Co. Karlsruhe, Germany. The compound was consisting of SiO_2:Al_2O_3 with mole ratio of 80:1 and a surface area of 780 m^2/g.

2.2. Thermogravimetric Analysis and Kinetic Study

Thermogravimetric analysis of lignin was performed without/with catalyst at heating rates of 15, 20, 25 and 30 °C/min from room temperature up to 600 °C using a thermogravimetric analyzer under N_2 flow of 20mL/min. The kinetic parameters were calculated from the resultant data using the following Kissinger equation [21,22]:

$$\ln\left[\frac{\beta}{T_m^2}\right] = \ln\left(\frac{A.R}{Ea}\right) - \frac{Ea}{RT_m} \quad (1)$$

where β, Ea, A, R and T_m stand for heating rate, activation energy, pre-exponential factor, universal gas constant and temperature at the rate peak maximum.

2.3. Pyrolysis Experiments and Products Characterization

Thermal and thermo-catalytic reactions were carried out at a wide temperature range in a furnace constructed locally. A detailed description of the pyrolysis assembly has already been given in our previous articles [23,24]; however, a schematic diagram of the same is reproduced here in Figure 1. A precisely weighed 5 g sample was taken in a reaction flask, put inside the furnace and heated at desired temperature by a coiled heater.The temperature of the furnace was monitored by a temperature controller. The flask was connected to a condenser, and the oil was collected in a vessel put inside the cold water. The pyrolysates, i.e., bio-oil, biochar and gas, were collected separately. The bio-oil was analyzed through GCMS (Shimadzu QP 2010 Plus). Helium at 2.0 mL/min was used as a carrier gas and split ratio of 1:18. A sample of about 1 µL was injected at an initial temperature of 60 °C with a holding time of 1 min, after which the temperature was increased at the rate of 4 °C/min to 265 °C with a holding time of 5 min. The column used for analysis was HP-5 Agilent. The peaks obtained from GC-MS chromatograph were then interpreted and identified using the NIST05 library of GC-MS. A scanning electron microscope (SEM) (JSM-5910, JEOL, Tokyo, Japan) and a transmission electron microscope (TEM) (JEM-2100 TEM, Japan) were used to characterize the biochar obtained from the pyrolysis in the presence and absence of the catalyst. For the SEM analysis, the biochar sample was mounted on the stub through a conducting carbon tape and sputtered with a gold layer by a coater. The SEM was fully evacuated and the sample was shifted to the machine for examining the morphology of the sample at 15 kV. A distance of 10 mm was maintained between the tip of the electron gun and biochar sample. For TEM analysis, the biochar was dissolved in acetone and sonicated for 10 min and then put one drop of sonicated colloidal solution on the formvar coated grid and air dried and then it was moved to the analysis chamber for examination at an accelerating voltage of 120 kV.

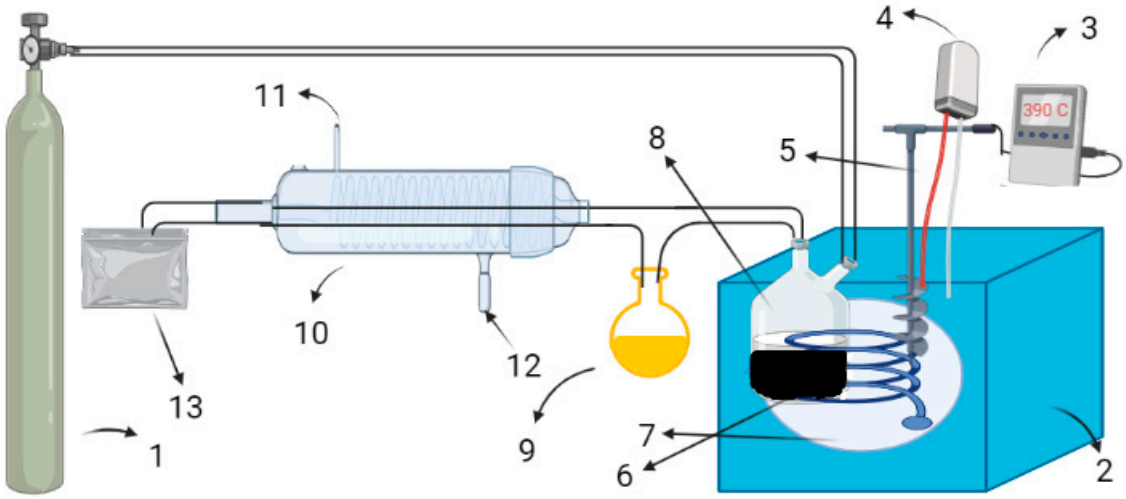

Figure 1. Experimental assembly for thermo-catalytic decomposition of lignin. 1. Nitrogen cylinder; 2. Insulation; 3. Display; 4. Power supply; 5. Thermocouple; 6. Coiled heater; 7. Salt bath; 8. Reaction vessel; 9. Oil collection vessel; 10. Condenser; 11. Water outflow; 12. Water inflow; 13. Gas collection bag.

3. Results and Discussion

3.1. Thermogravimetric Analysis and Kinetic Study

Thermogravimetric analysis of lignin was done without/with catalyst and the resultant data from TG/DTG plots was used for finding out kinetic parameters using Equation (1). The plots obtained are depicted in Figure 2, and the kinetic parameters calculated are presented in Table 1. The results show that Zeolite Y, hydrogen decreased the activation energy from 157.96 to 141.33 kJ/mol. These observations are in accord with reported results. Wang et al., [25] studied the pyrolysis of Douglas Fir with/without ZSM-5. Coats–Redfern approach was used for finding out kinetic parameters of the pyrolysis reaction. Authors observed that ZSM-5 speeded up the reaction and decreased the energy needed for the breakdown process.

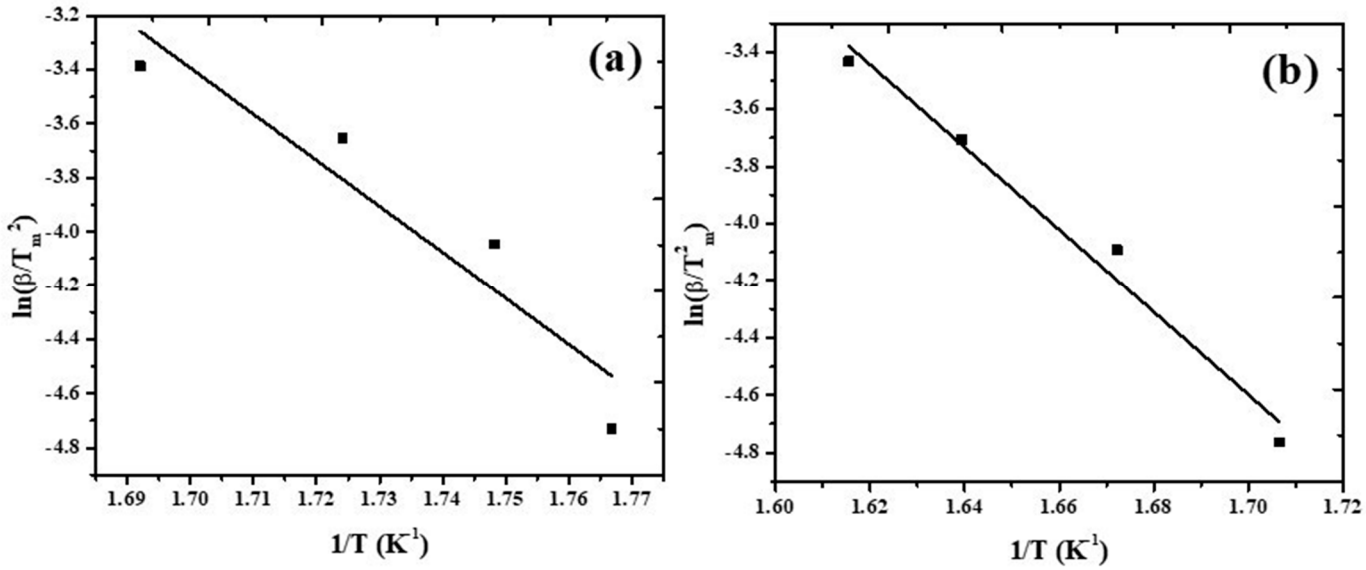

Figure 2. Kissinger plots constructed from (**a**) thermal and (**b**) thermo-catalytic decomposition of lignin.

Table 1. Determination of Kinetic parameters applying Kissinger equation.

Component	Thermal		Thermo-Catalytic	
	Ea (kJmol^{-1})	**A (min^{-1})**	**Ea (kJmol^{-1})**	**A (min^{-1})**
Lignin	157.96	2.66×10^{13}	141.33	2.17×10^{10}

Shrestha et al. [26] analyzed thermogravimetric analysis of lignin. The optimum temperature of mass decomposition was observed to be 345 °C and the char yield was 32% at 900 °C at heating rate of 5 K/min. When the rate was increased to 20 K/min, the optimum decomposition temperature was 341 °C, and the yield of biochar at 800 °C was 37.7%. Therefore, by increasing the heating rate, the optimum degradation temperature was decreased and the char yield was increased from 32 to 38%.

Nisar et al. [27] investigated the decomposition of peanut shells with/without termite hill at heating rates of 3, 12, 20, and 30 °C/min using Kissinger approach. The activation energies for hemicellulose, cellulose, and lignin were found 108.08, 116.4, and 182.91 kJ/mol for non-catalytic reaction and 66.512, 74.826 and 133.024 kJ/mol for catalytic reaction, respectively.

3.2. Characterization of Biochar

3.2.1. SEM Analysis

The surface features of biochar obtained from thermal and thermo-catalytic reactions were evaluated using a scanning electron microscope and transmission electron microscope. The SEM images are shown in Figure 3a,b. SEM analysis of non-catalyzed biochar reflects a smooth surface with a disc-like texture, while on the other hand the catalytic biochar was found to have a rough and uneven surface with multiple pores and irregular morphology. The application of biochar in energy storage supercapacitors requires a highly porous and larger surface area that could be produced by catalytic pyrolysis of lignin [28]. The interaction between lignin and the catalyst produced lump-like structures with a larger surface area and bigger diameter in the catalytic biochar. The use of the catalyst produced a strong morphological change that deformed the surface with a highly developed pore structure. Using textural examination, the lignin particles in biochar were further revealed to have been softened and merged into a mass of matrix and vesicles. These results agree with reported studies. Wang et al. [29] analyzed the textural properties of biochar produced from the exposure of alkali lignin to pyrolysis which showed the presence of irregularly fragmented surface pores that appeared to be broken and collapsed.

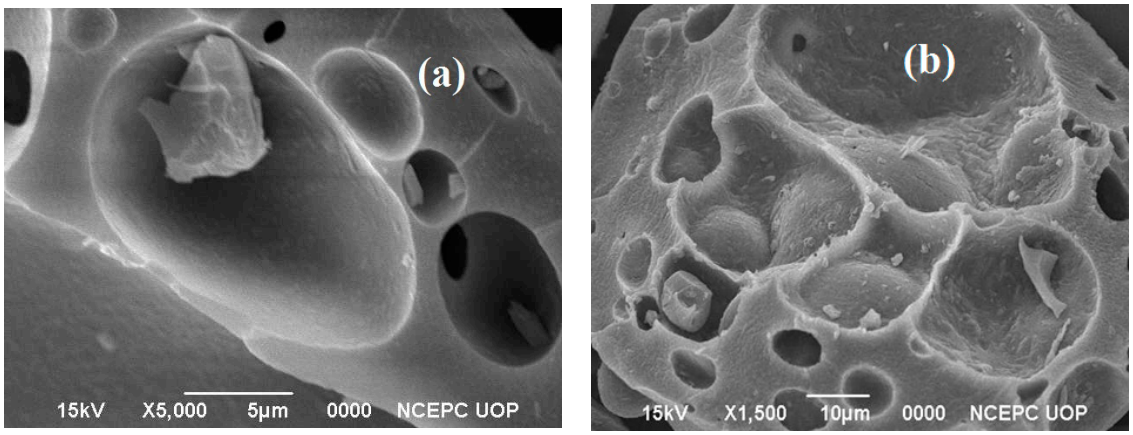

(**a**) (**b**)

Figure 3. SEM images of biochar obtained from (**a**) non-catalytic and (**b**) catalytic reactions.

3.2.2. TEM Analysis

The microstructure of lignin biochar was also analyzed using TEM. The TEM images (Figure 4a,b) obtained for non-catalytic biochar reflected a small surface area and an assembled structure due to the carbonization leading towards the fusion of the carbon skeleton. Biochar was observed to contain nanosized carbon particles with irregularly arranged fragments having submicron size and even surface area. The particle size was small and exhibited a highly rigid structure, while the catalytic biochar (Figure 4c,d) obtained showed different morphology due to the dispersion of the catalyst and, ultimately, an increased surface pore size due to agglomeration of nanosized carbon particles. The results agree well with reported literature. A TEM analysis of lignin biochar by Li et al. [30] showed similar agglomeration of carbon particles and the particles were evenly distributed in the carbon matrix.

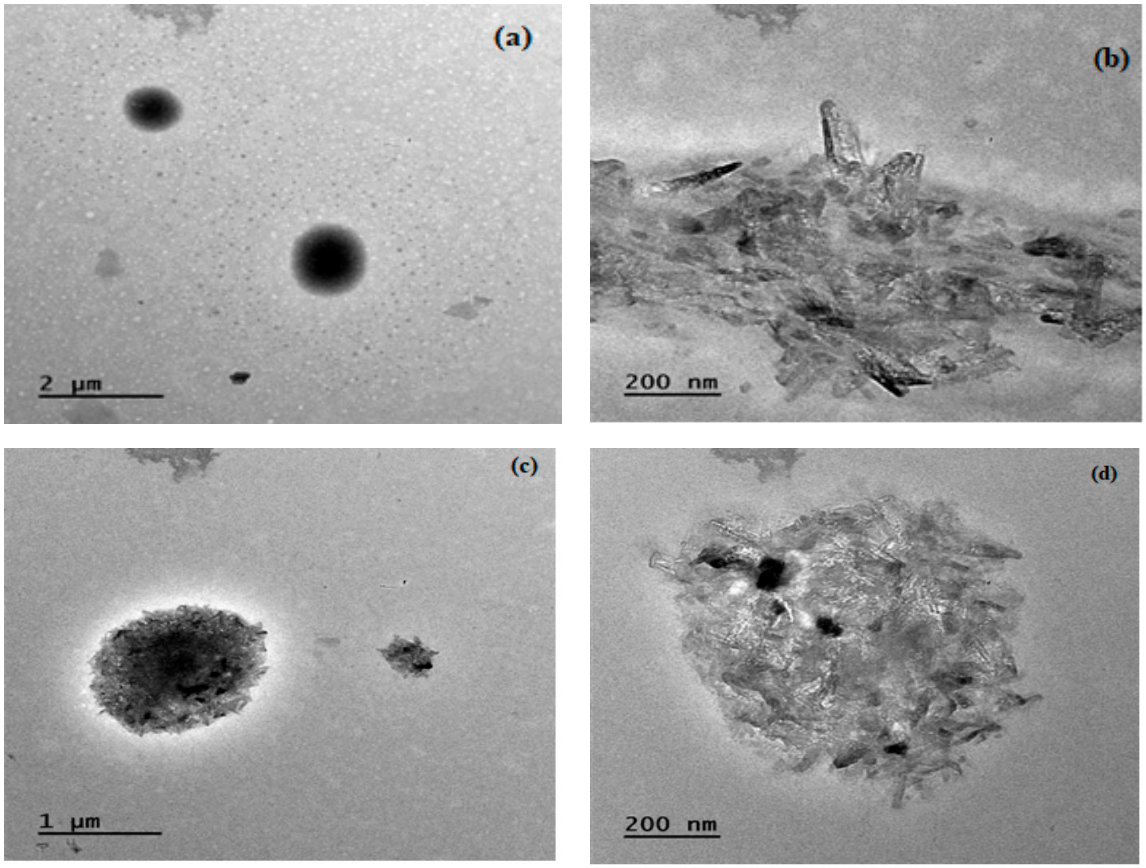

Figure 4. TEM images of biochar obtained from (**a**,**b**) non-catalytic and (**c**,**d**) catalytic pyrolysis.

3.3. Pyrolysis Experiments and GC/MS of Bio-Oil

In order to investigate the effect of temperature, pyrolysis experiments were carried out over wide range of temperature and the results are presented in Figure 5a,b. Pyrolysis carried out in the absence of catalyst produced maximum bio-oil at 410 °C (Figure 5a), whereas catalytic pyrolysis yielded maximum bio-oil at 390 °C (Figure 5b). This shows that the catalyst has dropped the maximum degradation temperature for maximum bio-oil yield. The subsequent breakdown caused a drop in the bio-oil beyond the optimal temperature and an increase in gases [31,32]. Additionally, a reduction in biochar was seen along with an increase in temperature. The trend is in consonance with earlier work. Nizamuddin et al. [33] studied the degradation of corn stalk and observed an increase in yield of oil with rise in temperature and then a decline was observed, a trend similar to our results. A similar pattern was also noted by Kalogiannis et al. [34]. They studied temperature effects on catalytic and thermal pyrolysis of lignin and observed an increase in

bio-oil with rise in temperature up to certain level and then a decrease in bio-oil was noted with increase in temperature. Jung et al. [35] investigated the influence of temperature on the formation of oil from the pyrolysis of lignin and observed maximum bio-oil of 31% at 670 °C. In another study, Jiang et al. [36] studied the influence of temperature on the pyrolytic products obtained from pyrolysis of lignin and recovered 18 wt% bio-oil at an optimized temperature of 600 °C having phenolic compounds in abundance. The influence of catalyst concentration on bio-oil yield is depicted in Figure 5c. As evident from the figure, with rise in catalyst loading from 1 to 3%, the bio-oil yield was observed to increase and then decline. This shows that rise in catalyst concentration favours bio-oil yield; however, it has adverse effects beyond 3% due to catalyst poisoning.

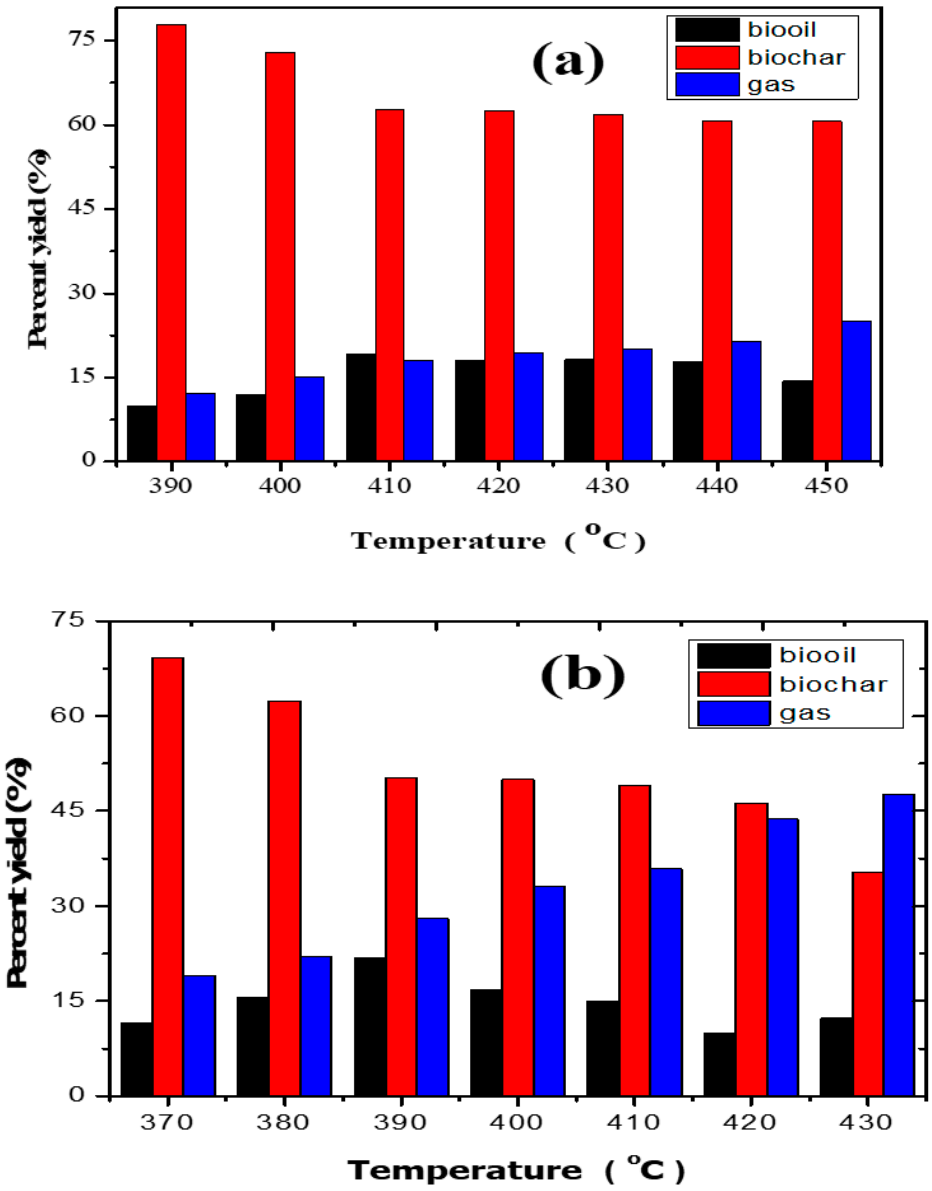

Figure 5. *Cont.*

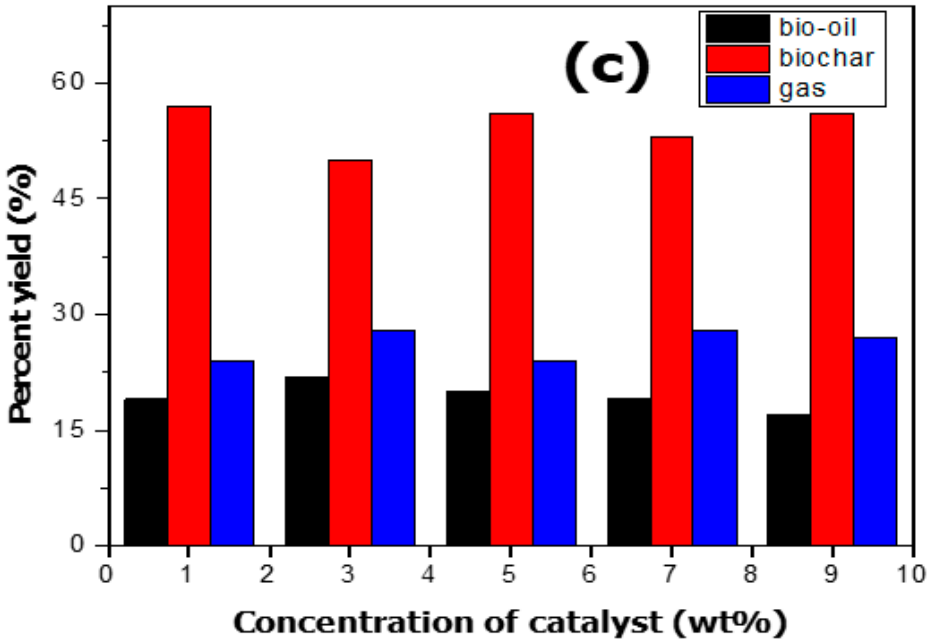

Figure 5. Product distribution from pyrolysis of lignin: (**a**) non-catalytic reaction; (**b**) catalytic reaction; and (**c**) effect of catalyst concentration.

The chromatogram of bio-oil collected from non-catalytic decomposition of lignin at optimized conditions as analyzed by GCMS is shown in Figure 6, and the identified components with their %area along with retention time are given in Table 2. The table indicates the presence of 58 components. Major components in the oil were Benzene, 1,1′-(1,3-propanediyl)bis, Phenol, 2-methoxy-, Naphthalene, 2-phenyl-, Benzene, 1,1′-(1,4-butanediyl)bis-, Benzene, 1,1′-(1-methyl-1,3-propan ediyl)bis, Benzene, 1,1′-(1,4-butanediyl)bis-, Vanillin, beta.-Phenyl propiophenone, and Diethanolamine with %area of 14.13, 8.47, 6.22, 3.66, 3.61, 3.60, 3.27 and 3.1%, respectively, which were produced as a result of lignin decomposition. These observations are in agreement with reported investigations [37]. Sharma et al., [11] pyrolyzed lignin between 150 and 550 °C and observed the relationship of lignin reactivity with the production of polycyclic aromatic hydrocarbons. Ateş et al. [37] examined the decomposition of sesame biomass to find out the influence of different parameters on the fuel production and their product distribution. Reaction temperature within the range of 400 to 700 °C was used for analysis under nitrogen-flow. The maximum bio-oil yield was noted to be 37.20 wt% of total weight at 550 °C and the bio-oil was found to comprise of branching hydrocarbons, alkenes, and alkanes.

GC/MS of the bio-oil collected from the catalyzed reaction of lignin was also performed and the results indicated that the zeolite has considerably reduced the oxygen-containing chemicals in the oil. The chromatogram is presented in Figure 7, and the different constituents present in the oil with their percent composition are presented in Table 3. The major constituents in the oil were observed as Benzene, 1,1′-(1,3-propanediyl)bis-, Phenol, 2-methoxy, Thiirane, methyl-, Naphthalene, 2-phenyl-, Naphthalene, 2-phenyl-, Vanillin, Apocynin, Benzene, 1,1′-(1-methyl-1,3-propane ediyl)bis-, Benzene, 1,1′-(1,4-butanediyl)bis-, m-Terphenyl, 1,2-Diphenylcyclopropane with % area of 33.3, 13.37, 12.18, 7.18, 4.47, 3.66, 3.62, 3.39, 3.35 and 3.14%, respectively. Besides these components, some other minor components were Butanoic acid, 2-methyl-, I-Stilbene, Benzene, (3-nitropropyl)-, Naphthalene, 2-(phenylmethyl)- and p-Terphenyl. GC/MS analysis also revealed that the presence of some value-added products has enhanced the quality of bio-oil. A comparative study of catalytic and non-catalytic decomposition shows that catalytic breakdown produced more benzene and phenol-like substances, which not only augmented the amount of bio-oil produced but also enhanced the value of oil. These observations agree well with some

reported work. Jeon et al. [38] studied catalytic degradation of biomass and observed an improvement in the quality of bio-oil as compared with oil recovered from an uncatalyzed pyrolysis process. Poplar wood catalytic cracking at 465 °C was explored by Mante et al. [39]. Their findings showed that the amount of Zeolite Y affected oil output and quality. The catalyst was also found efficient in refining the oil through elimination of some undesirable components. Ohra-aho and Linnekoski [40] studied Kraft lignin and Scots pine wood via pyrolysis using a variety of catalysts, including Zeolite Y, HZSM-5, and Pd/C. When compared with non-catalytic pyrolysis, both acid zeolite produced more aromatic hydrocarbons.

Hernando et al., [41] studied the decomposition of eucalyptus woodchips with ZSM-5 and Beta zeolites. Due to coke deposition on the catalyst and increased gas generation, the use of zeolite reduced the amount of bio-oil, however, the catalysts were able to lower the bio-oxygen in the oil's level and, therefore, improved the quality of the oil produced. Nisar et al., [42] carried out pyrolysis of sesame biomass in a salt bath in the presence of cobalt oxide. The GC/MS analysis indicated the oil consisting of 2-propanone, 2-pentanon-1-heptene, methanol, 2-propanone-1-hydroxy, 1-heptanol-2, 4-diethyl, 1-hexadecanesulfonyl chloride, 5-eicosene, 1-dodecanol-2-hexyl, 1-dodecanol-2-hexyl and nonadecyl trifluoroacetate, making the bio-oil a potential source of compounds with additional benefits.

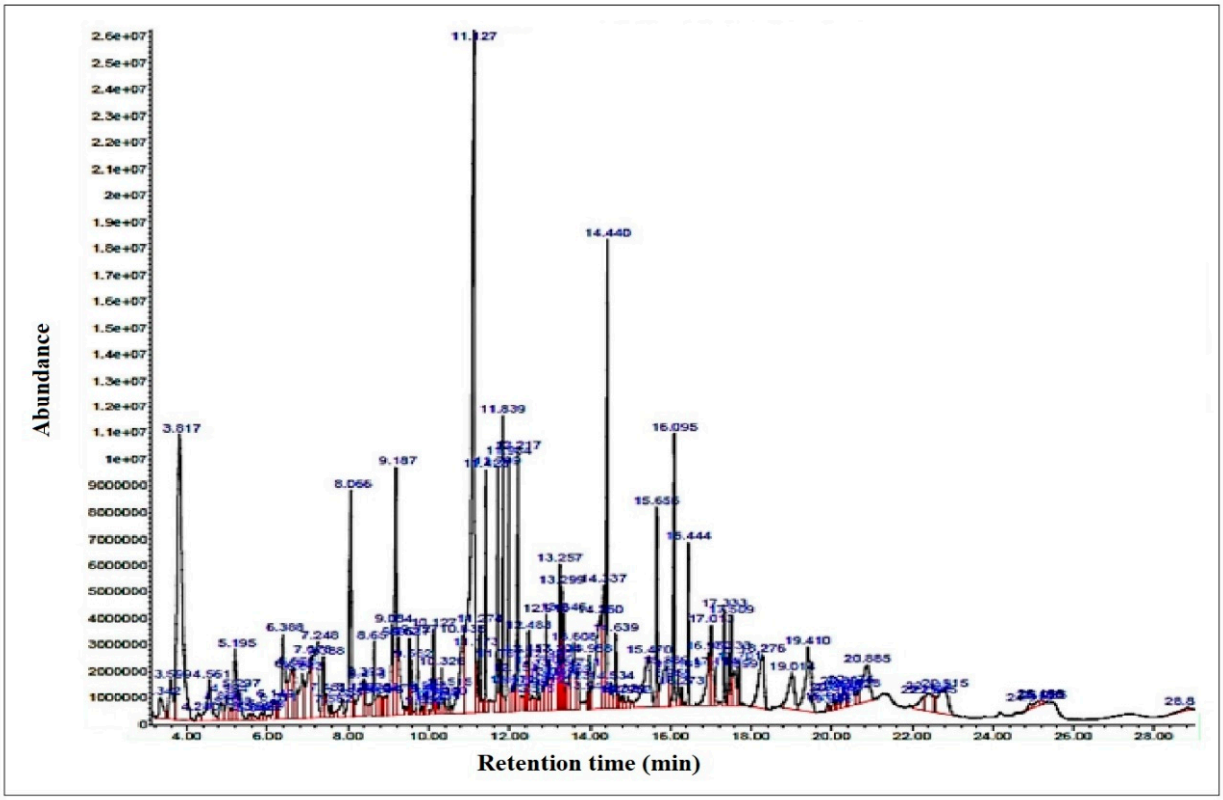

Figure 6. GCMS of oil collected from the pyrolytic decomposition of lignin in the absence of catalyst.

Table 2. Composition of bio-oil collected from lignin pyrolysis in the absence of catalyst.

S No	Retention Time	Compound Name	Chemical Formula	Mol.wt (g)	Area %
1	3.34	Phenol, 2-methyl-	$C_7H_6N_2O_5$	198.13	0.7
2	3.60	Phenol, 3-methyl-	C_7H_8O	108.14	0.89
3	3.82	Phenol, 2-methoxy-	$C_{10}H_{12}O_2$	170.16	8.47
4	4.27	Pentanoic acid, 2-methyl-, methyl ester	$C_7H_{14}O_2$	130.18	0.32
5	4.55	Benzene, 1,2-dimethoxy-	$C_8H_{10}O_2$	138.16	2.01
6	4.84	Phenol, 3-ethyl	$C_8H_{10}O$	122.16	0.52
7	5.19	Creosol	$C_8H_{10}O_2$	138.16	0.96
8	5.29	Catechol	$C_6H_6O_2$	110.10	0.68
9	5.55	Mequinol	$C_7H_{10}O_2$	124.13	0.28
10	5.64	Butanoic acid, 2-octyl ester	$C_{12}H_{24}O_2$	200.38	0.32
11	5.83	3,4-Dimethoxytoluene	$C_9H_{12}O_2$	152.19	0.29
12	5.92	Tricyclo [6.3.0.0(4,7)]undec-2-en-5-one, 9-[(2methoxyethoxy)methoxy]-8methyl-	$C_{16}H_{24}O_4$	280.36	0.31
13	6.14	1,2-Benzenediol, 3-methyl-	$C_7H_8O_2$	124.13	0.53
14	6.21	1-Propanol, 2-methyl-	$C_4H_{10}O$	74.12	0.14
15	6.38	Phenol, 4-ethyl-2-methoxy-	$C_9H_{12}O_2$	152.19	2.7
16	6.60	Propanoic acid	$C_3H_6O_2$	74.08	2.01
17	6.66	Diethylhydroxylamine	$C_4H_{11}NO$	89.14	0.99
18	6.86	Butanoic acid, 2-methyl-	$C_5H_{10}O_2$	102.13	2.08
19	7.07	N,N-Dimethylformamide diisopropyl acetal	$C_9H_{21}NO_2$	175.27	2.32
20	7.24	Diethanolamine	$C_4H_{11}NO_2$	105.13	3.02
21	7.39	Phenol, 2,6-dimethoxy-	$C_8H_{10}O_3$	154.16	0.57
22	7.45	Phenol, 2-methoxy-3-(2propenyl)-	$C_8H_{10}O_3$	154.26	0.27
23	7.58	Benzenemethanol,.alpha.ethyl-4-methoxy-	$C_{10}H_{14}O_2$	166.21	0.12
24	7.85	Pentanedioic acid, 2-methyl-	$C_7H_{12}O_4$	160.17	0.35
25	8.06	Vanillin	$C_8H_8O_3$	152.15	3.27
26	8.12	trans-Isoeugenol	$C_{10}H_{12}O$	164.20	0.21
27	8.39	1-(1-(Methylthio)propyl)-2propyldisulfane-	$C_7H_{16}S_3$	196.39	0.99
28	8.41	Diphenylmethane	$C_{13}H_{12}$	168.23	0.25
29	9.26	Butanoic acid, 3,3-dimethyl-, methyl ester	$C_{10}H_{20}O_2$	172.26	2.13
30	9.72	2-Propanone, 1-(4-hydroxy-3-methoxyphenyl)-	$C_{10}H_{12}O_4$	196.20	0.57
31	9.95	Butyrovanillone	$C_{11}H_{14}O$	194.22	0.13
32	10.12	Ethanone, 1-(3,4dimethoxyphenyl)-	$C_{10}H_{12}O_3$	180.20	0.5
33	10.17	1,1′-Biphenyl, 2-ethyl-	$C_{14}H_{14}$	182.26	0.11
34	10.32	1-Propanone, 1-(4-hydroxy-3-methoxyphenyl)-	$C_{10}H_{12}O_4$	196.19	0.85
35	10.38	4-Ethylbiphenyl	$C_{14}H_{14}$	182.26	0.87
36	10.51	Benzene, 4-butyl-1,2dimethoxy-	$C_{12}H_{18}O_2$	194.27	0.9
37	11.17	Benzenepropanol, 4hydroxy-3-methoxy-	$C_{10}H_{14}O$	182.21	0.93
38	11.27	1,2-Diphenylcyclopropane	$C_{15}H_{14}$	194.27	0.87

Table 2. *Cont.*

S No	Retention Time	Compound Name	Chemical Formula	Mol.wt (g)	Area %
39	11.84	3-(Benzylthio)acrylic acid, methyl ester	$C_{11}H_{12}O_2S$	208.28	2.75
40	11.12	Benzene, 1,1′-(1,3-propanediyl) bis	$C_{15}H_{16}$	196.28	14.13
41	11.42	Benzene, 1,1′-(1-methyl-1,3-propan ediyl) bis-	$C_{16}H_{18}$	210.31	3.61
42	11.98	1,2-Diphenylcyclopropane	$C_{15}H_{14}$	194.27	3.66
43	12.21	Benzene, 1,1′-(1,4-butanediyl) bis-	$C_{16}H_{18}$	210.31	3.6
44	13.25	Beta.-Phenyl propiophenone	$C_{16}H_{13}NO$	235.28	3.1
45	13.30	Naphthalene, 1-phenyl-	$C_{16}H_{12}$	204.27	0.92
46	14.44	Naphthalene, 2-phenyl-	$C_{16}H_{12}$	204.27	6.22
47	14.94	1,4-Diphenyl-1,3-butadiene benzene	$C_{16}H_{14}$	206.20	0.11
48	15.65	Naphthalene, 2-(phenylmethyl)-	$C_{17}H_{14}$	218.29	2.18
49	16.09	m-Terphenyl	$C_{18}H_{14}$	230.3	2.61
50	17.33	1-Methyl-2,4,5-trioxoimidazolidine	$C_4H_4N_2O_3$	128.09	0.96
51	17.43	n-Butanol, 2-[3chlorophenoxy]-	$C_{10}H_{13}ClO_2$	200.66	0.48
52	17.50	L-Ornithine,N,N′-bis(methoxycarbo nyl)-, methyl ester	$C_5H_{12}N_2O_2$	132.26	0.95
53	18.27	Cyclononasiloxane, octadecamethyl-	$C_{18}H_{54}O_9Si_9$	667.4	2.59
54	19.41	Cyclooctasiloxane, hexadecamethyl-	$C_{16}H_{48}O_8Si_8$	593.2	2.87
55	19.01	2-Aminophenol,N,O-bis(pentafluoropropionyl)-	C_6H_7NO	109.13	2.16
56	20.88	Tetracosamethyl-cyclododecasiloxan	$C_{24}H_{72}O_{12}Si_{12}$	889.8	2.41
57	22.29	Benzamide,4-methoxy-N-[4-(1-methylcyclopropyl)phenyl]-	$C_{10}H_{13}NO_2$	179.22	0.73
58	25.25	Tetracosamethylcyclododecasiloxan	$C_{24}H_{72}O_{12}$	889.84	0.53

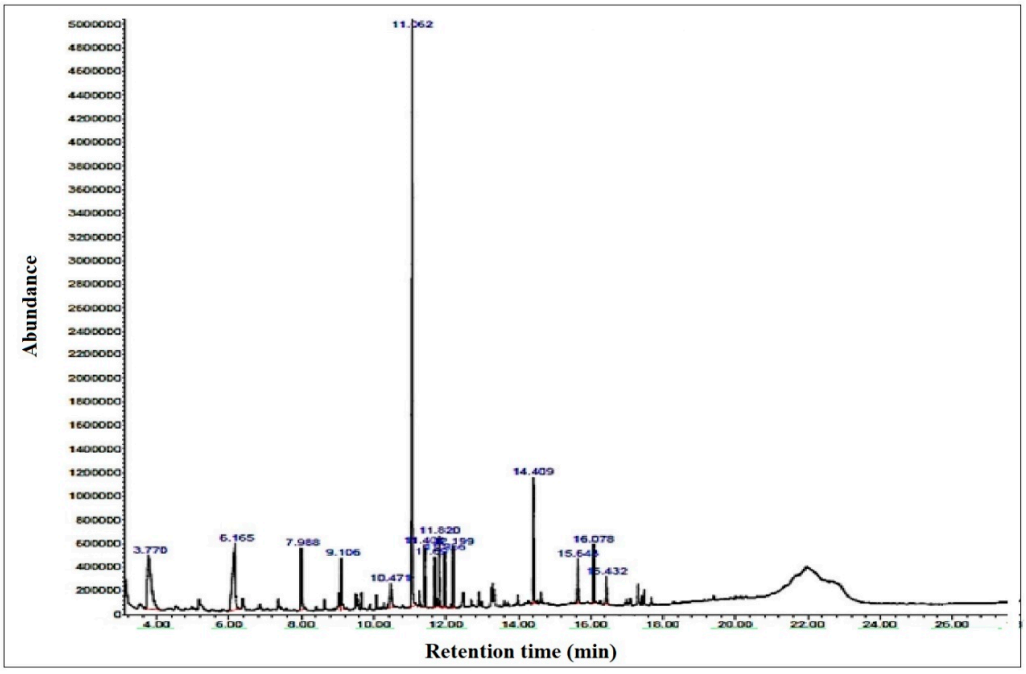

Figure 7. GCMS of oil collected from the pyrolytic decomposition of lignin in the presence of catalyst.

Table 3. Composition of bio-oil collected from lignin pyrolysis in the presence of catalyst.

S.No	Retention Time	Compound Name	Chemical Formula	Mol. Wt. (g)	% Area
1	3.768	Phenol, 2-methoxy	$C_7H_8O_2$	124.13	13.37s
2	6.165	Thiirane, methyl-	C_3H_6S	74.14	12.18
3	7.991	Vanillin	$C_8H_8O_3$	152.15	4.47
4	9.107	Apocynin	$C_9H_{10}O_3$	166.17	3.66
5	10.468	Butanoic acid, 2-methyl-	$C_5H_{10}O_2$	102.13	2.40
6	11.063	Benzene, 1,1′-(1,3-propanediyl) bis-	$C_{18}H_{22}$	238.40	33.30
7	11.40	Benzene, 1,1′-(1-methyl-1,3-propane ediyl)bis-	$C_{16}H_{18}$	210.31	3.62
8	11.69	(E)-Stilbene	$C_{14}H_{12}$	180.25	2.75
9	11.81	Benzene, (3-nitropropyl)-	$C_9H_{11}NO_2$	165.19	2.92
10	11.96	1,2-Diphenylcyclopropane	$C_{15}H_{14}$	194.27	3.14
11	12.20	Benzene,1,1′-(1,4 butanediyl)bis-	$C_{16}H_{18}$	210.31	3.39
12	14.41	Naphthalene, 2-phenyl-	$C_{16}H_{12}$	204.27	7.18
13	15.64	Naphthalene, 2-(phenylmethyl)-	$C_{17}H_{14}$	210.29	2.52
14	16.07	m-Terphenyl	$C_{18}H_{14}$	230.30	3.35
15	16.43	p-Terphenyl	$C_{18}H_{14}$	230.30	1.75

4. Conclusions

Thermo-catalytic decomposition of lignin was performed in a locally made pyrolysis chamber. The bio-oils collected as a result of catalyzed and non-catalyzed pyrolytic reactions were studied using gas chromatography mass spectrometry. The bio-oil recovered from catalytic pyrolysis was found to be superior in quality due to the presence of fuel range hydrocarbons as compared to the bio-oil formed from non-catalytic pyrolysis. For the kinetic study, both the samples were subjected to thermogravimetric analysis at various heating rates and activation energy was calculated using Kissinger equation for both catalytic and non-catalytic decomposition reactions and found to be 141.33 kJ/mol and 157.96 kJ/mol, respectively. From the results, it has been concluded that Zeolite Y, hydrogen demonstrated to be an efficient catalyst as it has not only decreased the activation energy of the pyrolysis reaction but also enhanced the quality of bio-oil. The presence of some fuel range hydrocarbons in the bio-oil produced from the catalyzed reaction has bright prospects for use as commercial fuel if upgraded properly.

Author Contributions: G.A., writing, results and analysis. M.A. and F.M., investigation, methodology, writing—original draft. J.N., conceptualization, funding acquisition, resources, project administration. A.S., visualization, writing—review and editing. S.M., review and editing. S.T.H., review and editing. All authors have read and agreed to the published version of the manuscript.

Funding: Jan Nisar acknowledges the support of the Higher Education Commission of Pakistan through grant No. 20-1491.

Conflicts of Interest: The authors have no conflict of interest.

References

1. Raza, M.A.; Aman, M.M.; Rajpar, A.H.; Bashir, M.B.A.; Jumani, T.A. Towards Achieving 100% Renewable Energy Supply for Sustainable Climate Change in Pakistan. *Sustainability* **2022**, *14*, 16547. [CrossRef]
2. Potrč, S.; Čuček, L.; Martin, M.; Kravanja, Z. Sustainable renewable energy supply networks optimization—The gradual transition to a renewable energy system within the European Union by 2050. *Renew. Sustain. Energy Rev.* **2021**, *146*, 111186. [CrossRef]
3. Ioelovich, M. Recent findings and the energetic potential of plant biomass as a renewable source of biofuels—A review. *Bioresources* **2015**, *10*, 1879–1914.

4. Ioelovich, M. *Plant Biomass as a Renewable Source of Biofuels and Biochemicals*; LAP LAMBERT Academic Publishing: Sunnyvale, CA, USA, 2013.
5. Ahmed, M.M.; Nasri, N.S.; Hamza, D.U. Biomass as a renewable source of chemicals for industrial applications. *Int. J. Eng. Sci. Technol.* **2012**, *4*, 721–730.
6. Włodarczyk, B.; Firoiu, D.; Ionescu, G.H.; Ghiocel, F.; Szturo, M.; Markowski, L. Assessing the Sustainable Development and Renewable Energy Sources Relationship in EU Countries. *Energies* **2021**, *14*, 2323. [CrossRef]
7. Nisar, J.; Ullah, N.; Awan, I.A.; Iqbal, M.; Khan, T.A. Pyrolysis–Gas Chromatography of Sugar Beet Bagasse. *Waste Biomass Valoriz.* **2015**, *7*, 79–85. [CrossRef]
8. Taarning, E.; Osmundsen, C.M.; Yang, X.; Voss, B.; Andersen, S.I.; Christensen, C.H. Zeolite based biomass conversion to fuels and chemicals. *Energy Environ. Sci.* **2011**, *4*, 793–804. [CrossRef]
9. Galadima, A.; Muraza, O. In situ fast pyrolysis of biomass with zeolite catalysts for bioaromatics/gasoline production: A review. *Energy Convers. Manag.* **2015**, *105*, 338–354. [CrossRef]
10. Jiang, G.; Nowakowski, D.J.; Bridgwater, A.V. A systematic study of the kinetics of lignin pyrolysis. *Thermochim. Acta* **2010**, *498*, 61–66. [CrossRef]
11. Sharma, R.K.; Wooten, J.B.; Baliga, V.L.; Lin, X.; Chan, W.G.; Hajaligol, M.R. Characterization of chars from pyrolysis of lignin. *Fuel* **2004**, *83*, 1469–1482. [CrossRef]
12. Kawamoto, H. Lignin pyrolysis reactions. *J. Wood Sci.* **2017**, *63*, 117–132. [CrossRef]
13. Mu, W.; Ben, H.; Ragauskas, A.; Deng, Y. Lignin Pyrolysis Components and Upgrading—Technology Review. *BioEnergy Res.* **2013**, *6*, 1183–1204. [CrossRef]
14. Liu, Q.; Wang, S.; Zheng, Y.; Luo, Z.; Cen, K. Mechanism study of wood lignin pyrolysis by using TG–FTIR analysis. *J. Anal. Appl. Pyrolysis* **2008**, *82*, 170–177. [CrossRef]
15. Li, M.; Pu, Y.; Ragauskas, A.J. Current Understanding of the Correlation of Lignin Structure with Biomass Recalcitrance. *Front. Chem.* **2016**, *4*, 45. [CrossRef]
16. Vanholme, R.; Morreel, K.; Ralph, J.; Boerjan, W. Lignin engineering. *Curr. Opin. Plant Biol.* **2008**, *11*, 278–285. [CrossRef] [PubMed]
17. Novaes, E.; Kirst, M.; Chiang, V.; Winter-Sederoff, H.; Sederoff, R. Lignin and Biomass: A Negative Correlation for Wood Formation and Lignin Content in Trees. *Plant Physiol.* **2010**, *154*, 555–561. [CrossRef] [PubMed]
18. Watkins, D.; Nuruddin, M.; Hosur, M.; Tcherbi-Narteh, A.; Jeelani, S. Extraction and characterization of lignin from different biomass resources. *J. Mater. Res. Technol.* **2015**, *4*, 26–32. [CrossRef]
19. Lim, H.Y.; Yusup, S.; Loy, A.C.M.; Samsuri, S.; Ho, S.S.K.; Manaf, A.S.A.; Lam, S.S.; Chin, B.L.F.; Acda, M.N.; Unrean, P.; et al. Review on Conversion of Lignin Waste into Value-Added Resources in Tropical Countries. *Waste Biomass Valoriz.* **2020**, *12*, 5285–5302. [CrossRef]
20. Ioelovich, M. Methods for determination of chemical composition of plant biomass. *J. SITA* **2015**, *17*, 208–214.
21. Nisar, J.; Waris, S.; Shah, A.; Anwar, F.; Ali, G.; Ahmad, A.; Muhammad, F. Production of Bio-Oil from De-Oiled Karanja (*Pongamia pinnata* L.) Seed Press Cake via Pyrolysis: Kinetics and Evaluation of Anthill as the Catalyst. *Sustain. Chem.* **2022**, *3*, 345–357. [CrossRef]
22. Blaine, R.L.; Kissinger, H.E. Homer Kissinger and the Kissinger equation. *Thermochim. Acta* **2012**, *540*, 1–6. [CrossRef]
23. Nisar, J.; Rahman, A.; Ali, G.; Shah, A.; Farooqi, Z.H.; Bhatti, I.A.; Iqbal, M.; Rehman, N.U. Pyrolysis of almond shells waste: Effect of zinc oxide on kinetics and product distribution. *Biomass Convers. Biorefin.* **2020**, *12*, 2583–2595. [CrossRef]
24. Nisar, J.; Sharaf, M.; Ali, G.; Farooqi, Z.H.; Iqbal, M.; Khan, S. Pyrolysis of juice-squeezed grapefruit waste: Effect of nickel oxide on kinetics and bio-oil yield. *Int. J. Environ. Sci. Technol.* **2022**, *19*, 10211–10222. [CrossRef]
25. Wang, L.; Lei, H.; Liu, J.; Bu, Q. Thermal decomposition behavior and kinetics for pyrolysis and catalytic pyrolysis of Douglas fir. *RSC Adv.* **2018**, *8*, 2196–2202. [CrossRef]
26. Shrestha, B.; Le Brech, Y.; Ghislain, T.; Leclerc, S.; Carré, V.; Aubriet, F.; Hoppe, S.; Marchal, P.; Pontvianne, S.; Brosse, N.; et al. A Multitechnique Characterization of Lignin Softening and Pyrolysis. *ACS Sustain. Chem. Eng.* **2017**, *5*, 6940–6949. [CrossRef]
27. Nisar, J.; Ahmad, A.; Ali, G.; Rehman, N.U.; Shah, A.; Shah, I. Enhanced Bio-Oil Yield from Thermal Decomposition of Peanut Shells Using Termite Hill as the Catalyst. *Energies* **2022**, *15*, 1891. [CrossRef]
28. Xiu, S.; Shahbazi, A.; Li, R. Characterization, Modification and Application of Biochar for Energy Storage and Catalysis: A Review. *Trends Renew. Energy* **2017**, *3*, 86–101. [CrossRef]
29. Wang, W.; Liu, Y.; Wang, Y.; Liu, L.; Hu, C. Effect of nickel salts on the production of biochar derived from alkali lignin: Properties and applications. *Bioresour. Technol.* **2021**, *341*, 125876. [CrossRef]
30. Li, C.; Hayashi, J.-I.; Sun, Y.; Zhang, L.; Zhang, S.; Wang, S.; Hu, X. Impact of heating rates on the evolution of function groups of the biochar from lignin pyrolysis. *J. Anal. Appl. Pyrolysis* **2021**, *155*, 105031. [CrossRef]
31. Westerhof, R.J.M.; Brilman, D.W.F.; van Swaaij, W.P.M.; Kersten, S.R.A. Effect of Temperature in Fluidized Bed Fast Pyrolysis of Biomass: Oil Quality Assessment in Test Units. *Ind. Eng. Chem. Res.* **2010**, *49*, 1160–1168. [CrossRef]
32. Demirbas, A. Effect of temperature on pyrolysis products from four nut shells. *J. Anal. Appl. Pyrolysis* **2006**, *76*, 285–289. [CrossRef]
33. Nizamuddin, S.; Baloch, H.A.; Mubarak, N.M.; Riaz, S.; Siddiqui, M.T.H.; Takkalkar, P.; Tunio, M.M.; Mazari, S.; Bhutto, A.W. Solvothermal Liquefaction of Corn Stalk: Physico-Chemical Properties of Bio-oil and Biochar. *Waste Biomass Valoriz.* **2018**, *10*, 1957–1968. [CrossRef]

34. Kalogiannis, K.G.; Stefanidis, S.D.; Michailof, C.M.; Lappas, A.A.; Sjöholm, E. Pyrolysis of lignin with 2DGC quantification of lignin oil: Effect of lignin type, process temperature and ZSM-5 in situ upgrading. *J. Anal. Appl. Pyrolysis* **2015**, *115*, 410–418. [CrossRef]
35. Jung, K.A.; Nam, C.W.; Woo, S.H.; Park, J.M. Response surface method for optimization of phenolic compounds production by lignin pyrolysis. *J. Anal. Appl. Pyrolysis* **2016**, *120*, 409–415. [CrossRef]
36. Jiang, G.; Nowakowski, D.J.; Bridgwater, A.V. Effect of the Temperature on the Composition of Lignin Pyrolysis Products. *Energy Fuels* **2010**, *24*, 4470–4475. [CrossRef]
37. Ateş, F.; Pütün, E.; Pütün, A.E. Fast pyrolysis of sesame stalk: Yields and structural analysis of bio-oil. *J. Anal. Appl. Pyrolysis* **2004**, *71*, 779–790. [CrossRef]
38. Jeon, M.-J.; Jeon, J.-K.; Suh, D.J.; Park, S.H.; Sa, Y.J.; Joo, S.H.; Park, Y.-K. Catalytic pyrolysis of biomass components over mesoporous catalysts using Py-GC/MS. *Catal. Today* **2013**, *204*, 170–178. [CrossRef]
39. Mante, O.D.; Agblevor, F.A.; McClung, R. Fluid catalytic cracking of biomass pyrolysis vapors. *Biomass Convers. Biorefin.* **2011**, *1*, 189–201. [CrossRef]
40. Ohra-Aho, T.; Linnekoski, J. Catalytic pyrolysis of lignin by using analytical pyrolysis-GC–MS. *J. Anal. Appl. Pyrolysis* **2015**, *113*, 186–192. [CrossRef]
41. Hernando, H.; Moreno, I.; Fermoso, J.; Ochoa-Hernández, C.; Pizarro, P.; Coronado, J.M.; Cejik, J.; Serrano, D.P. Biomass catalytic fast pyrolysis over hierarchical ZSM-5 and Beta zeolites modified with Mg and Zn oxides. *Biomass Convers. Biorefin.* **2017**, *7*, 289–304. [CrossRef]
42. Nisar, J.; Ali, F.; Malana, M.A.; Ali, G.; Iqbal, M.; Shah, A.; Bhatti, I.A.; Khan, T.A.; Rashid, U. Kinetics of the pyrolysis of cobalt-impregnated sesame stalk biomass. *Biomass Convers. Biorefin.* **2020**, *10*, 1179–1187. [CrossRef]